Photo- and Thermo-stable Luminescent Beads Composed of Eu(III) Complexes and PMMA for Enhancement of Silicon Solar Cell Efficiency

Hisataka Kataoka[a], Tetsuo Kitano[a], Toshiki Takizawa[a], Yuichi Hirai[b], Takayuki Nakanishi[b], Yasuchika Hasegawa[b]*

a Bridgestone Corporation, 1,Kashio-Cho,Totsuka-Ku,Yokohama 244-8510,Japan

b Faculty of engineering, Hokkaido University, Kita 13 Nishi 8, Kita-ku, Sapporo 060-8628, Japan

Keywords:

lanthanide, europium, complex, solar cell

Corresponding author.

Tel./fax. +81 11 706 7114

E-mail address:

hasegaway@eng.hokudai.ac.jp

Abstract

Photo- and thermo-stable luminescent beads composed of $Eu(hfa)_3(TPPO)_2$ (hfa: hexafluoroacetylacetonate, TPPO: triphenylphosphine oxide) and PMMA (polymethylmethacryrate), $Eu(hfa)_3(TPPO)_2$-beads, have been reported for improvement of energy conversion efficiency on silicon solar cell. The photophysical properties of $Eu(hfa)_3(TPPO)_2$ and compared $Eu(tta)_3(TPPO)_2$ (tta: trifluoromethyl- thienylacetylacetonate) are characterized by the emission quantum yield, the emission lifetime, the radiative and the non-radiative rate constants. Photo- and thermo-stability of the beads with Eu(III) complexes in EVA (Ethylene Vinyl Acetate) are estimated under UV irradiation (Xenon lamp: $60W/m^2$) and highly temperature (120 ^oC). The stability of the $Eu(hfa)_3(TPPO)_2$-beads for industrial application was calculated to be ten years under air condition. Energy conversion efficiency of silicon solar cells attached EVA films with $Eu(hfa)_3(TPPO)_2$-beads increased approximately 2%(10% → 10.2%) compared with EVA films contained with UV absorber. Photo- and thermo-stable $Eu(hfa)_3(TPPO)_2$-beads for silicon solar cells are demonstrated for the first time.

Introduction

There has been significant recent interest in the development of luminescent metal complexes for applications such as optical materials, organic LED, and fluorescent sensor for medical use [1-3]. In particular, lanthanide complexes with characteristic emission caused from 4f orbital have been regarded as attractive luminescent materials for use in electroluminescent (EL) devices, laser, and luminescent bio-sensing applications [4-6]. Luminescent lanthanide complexes composed of lanthanide ions and organic ligand with π-conjugated system provide large absorption cross-section at the ligand-absorption bands and characteristic large stokes shift between the excitation and the emission bands. Bünzli and Parker have reviewed various types of luminescent lanthanide complexes [7]. We have also reported strong-luminescent Eu(III), Tb(III), Sm(III), Yb(III) and Nd(III) complexes with large emission quantum yield and radiative rate constants, recently [8]. A large number of scientific studies on luminescence lanthanide complexes have been reported [9].

We here focus on photovoltaic application for enhancement of solar cell efficiency using strong-Luminescent Eu(III) complexes. First photovoltaic application using Eu(III) and Tb(III) bipyridyl complexes in polymer films have been reported by G. Adachi and K. Machida [10]. Recently, Fukuda has described wave-converter layer composed of sol-gel glass with encapsulated $Eu(tta)_3phen$ (tta: trifluoromethylthienylacetylacetonate, phen:1-10,phenanthroline) for silicon solar cell [11]. Segawa has provided EVA (Ethylene Vinyl Acetate) films including ((Eu(1-naphthoic $acid)_3phen$ (phen:1-10,phenanthroline) complex for wave-converter of silicon solar cells, and observed effective improvement of the solar cells (from 254.3KWh to257.2 KWh) [12]. Kawano has also described CdTe solar cell modules with EVA film containing ($(Eu(tmhd)_3$ (tmhd:tris(2,2,6,6-tetramethyl-3,5heptanedionate) complexes for enhancement of photo-energy conversion efficiency at around 320-450nm [13]. At the present stage, EVA thin films containing

Eu(III) complexes are expected to be a promising material for improvement of silicon and CdTe solar cells.

Previous Eu(III) complex in EVA films, $Eu(tta)_3$, is generally composed of Eu(III) ion and diketonate ligands with thienyl groups, tta ligands. The thienyl groups in tta ligand decomposed under air because of their oxidation [14]. On the other hand, transparent EVA film as a matrix for fixation of Eu(III) complexes also produces acetic acid under water at high temperature (hydrolysis reaction). The acidic materials promote decomposition of luminescent Eu(III) complexes in EVA. From these reasons, development of air-, thermal- and photo-stable structure of Eu(III) complexes in EVA would be required for future application in solar cells.

To protect Eu(III) complexes from oxygen, water, and acidic materials, we designed novel air-stable Eu(III) complex covered with acid-resistant polymer matrix. In this study, we here report novel luminescent polymer beads composed of $Eu(hfa)_3(TPPO)_2$ (hfa: hexafluoroacetylacetonate, TPPO: triphenylphosphine oxide, Fig. 1a) and PMMA(Polymethylmethacrylate) for enhancement of energy conversion efficiency of silicon solar cells. The $Eu(hfa)_3(TPPO)_2$ without thienyl groups shows strong photo-, air-, and thermo-stable luminescence excited at around 300nm. We also prepared $Eu(tta)_3(TPPO)_2$ for comparison of thienyl units with trifluoromethyl groups under irradiation and highly temperature (Fig. 1b). The emission properties of $Eu(hfa)_3(TPPO)_2$ and $Eu(tta)_3(TPPO)_2$ were characterized by the emission quantum yields, the emission lifetimes, radiative and non-radiative rate constants. In order to protect around the Eu(III) complexes from acid materials, luminescent PMMA beads including Eu(III) complexes, $Eu(hfa)_3(TPPO)_2$-beads and $Eu(tta)_3(TPPO)_2$-beads, were prepared by the polymerization of methyl methacrylate with Eu(III) complexes and AIBN under water at 95 ^oC (Fig. 1 c). Stability of luminescent beads was evaluated under UV irradiation (Xenon lamp: 60W/m^2) and highly temperature (120 ^oC). We also report enhancement of short-circuit current efficiency of solar cell module with $Eu(hfa)_3(TPPO)_2$-beads.

Photo- and thermo-stable EVA thin film with $Eu(hfa)_3(TPPO)_2$-beads for improvement of silicon solar cell have been demonstrated for the first time.

2. Experimental

2.1. Apparatus

FT-IR measurements were performed at room temperature by Perkin-Elmer system 2000 FT-IR spectrometer. ^1H NMR measurements were measured using JEOL AL-300 spectrometer (400MHz). Chemical shifts are reported in ppm and are referenced to an internal tetramethylsilane (TMS) standard for ^1H NMR spectroscopy. Sort-circuit currents of solar cell module under irradiation were obtained with SAN-EI ELECTRIC XES-220CS1 solar simulator. Photo-stability of solar sell module was measured by using SUGA TEST INSTRUMENTS X75 Xenon TESTER (63 ^oC, 60W/ m^2).

2.2. Preparation of $Eu(hfa)_3(TPPO)_2$

Methanol (100 mL) containing $Eu(hfa\text{-}H)_3(H_2O)_2$ (4.28 g, 6 mmol) and triphenylphospine oxide (TPPO) (2.78 g, 10 mmol) was refluxed under stirring for 12 hours. The reaction mixture was concentrated using a rotary evaporator. Reprecipitation by addition of excess hexane solution produced crude crystals, which were washed in toluene several times. Recrystallization from hot toluene/cyclohexane gave white needle crystals ($Eu(hfa)_3(TPPO)_2$). Yield: 74%. ^1H NMR (400 MHz, CD_3-$COCD_3$, TMS) : δ 5.41 (s, 3H : -CH), δ = 7.62-7.66 (m, 12H : Ar), 7.79-7.83 (m, 6H : Ar), 8.65 (s, 12H : Ar) ppm. Selected IR (KBr): ν = 1125 (P=O), 1150-1250 (-CF), 1650 (-C = O) cm^{-1}. Elemental analysis calculated (%) for $C_{51}H_{36}EuF_{18}O_8P_2$: C, 46.07 , H, 2.50; found: C, 46.03, H, 2.51.

2.3. Preparation of $Eu(tta)_2(TPPO)_2$

4,4,4-trifluoro-1-(2-thienyl)-1,3-butanedione (tta, 0.67 g, 3.0 mmol), triphenylphosphine oxide (TPPO, 0.56 g, 2.0 mmol)) and 2,2′-iminodiethanol (0.32 g, 3.0 mmol) were dissolved in 40 ml of isopropanol. To this solution, a solution obtained by dissolving europium chloride (III) hexahydrate (0.37 g, 1 mmol) in 20 ml of a mixed solvent of water/isopropanol (1/4) was added dropwise at room temperature taking 2 hours, and stirring was further continued at room temperature for 1 hour. A precipitate formed was filtered by suction, and washed with water and isopropanol. The resulting light yellow powder was dried under vacuum at 50° C. Yield: 72%. ^{1}H NMR (400 MHz, CD_3-$COCD_3$, TMS) : δ = 5.9 (s, 3H : -CH), δ 6.31-6.35 (m, 12H : Ar), 6.97-6.99 (m, 12H : Ar), 7.65-7.83 (m, 24H : Ar). Selected IR (KBr): ν = 1121 (P=O), 1150-1300 (-CF), 1610 (-C=O) cm^{-1}. Elemental analysis calculated (%) for $C_{60}H_{45}EuF_9O_8P_2S_3$: C, 52.52, H, 3.09; found: C, 51.82, H, 3.01.

2.4. Preparation of PMMA beads with $Eu(hfa)_3(TPPO)_2$ or $Eu(tta)_3(TPPO)_2$, $Eu(hfa)_3(TPPO)_2$-beads or $Eu(tta)_3(TPPO)_2$-beads

$Eu(hfa)_3(TPPO)_2$ (0.3 g) was dissolved methyl Methacrylate (MMA 100 g), 2,2'-Azobisisobutyronitrile (AIBN, 0.3 g), benzoyl peroxide (BPO 0.2 g) and ethylenoxidedimethacrylate (10 g), at room temperature. The liquid solution was added to deionized water, stirring and reacting at 55 ^oC for 1h and 95 ^oC for 3 hours by suspension polymerization method. IR (KBr): ν = 1123 (-CF), 1130 (P=O), 1700 (-C = O) cm^{-1}. PMMA beads containing $Eu(tta)_2(TPPO)_3$ was also obtained using the same method.

2.5. Preparation of EVA films containing $Eu(hfa)_3(TPPO)_2$-beads or $Eu(tta)_3(TPPO)_2$-beads

Triarylisocyanate (0.5 g), t-butyl peroxy-2-ethylhexyl monocarbonate (0.5 g), silane coupling

agent (0.3 g), and PMMA beads including Eu(III) complex (0.5 g) were dispersed with EVA resin (copolymer: ethylene: vinyl acetate contents = 74: 26, 100g), before kneading process. The dispersion containing with them was kneaded at temperature 75 ^{o}C, and then EVA films were prepared by calendaring process. Thickness of the EVA films were found to be 0.5 mm.

2.6. Preparation of Stacked materials composed of EVA film and glass plates for experiments of photo- and thermo-stabilities

EVA film containing PMMA beads (thickness = 0.5 mm) was sandwiched by Glass plates (low iron glass: thickness = 3 mm). Sample heating is used by Module laminator equipped with hot plate in a vacuum environment, the rubber diaphragm for pressing. The Stacked materials composed of EVA film and glass plates were heated to 150 ^{o}C on the hot plate under vacuum for 5 minutes to removing air in the Stacked materials, and pressed for 20 min using Module laminator (LM-110×160-S, NPC Incorporated) for crosslinking EVA polymer . The prepared glass was used for estimation of emission stability under UV irradiation.

2.7. Preparation of silicon solar modules

A glass plate (low iron glass: thickness = 3mm), solar cell sealing film containing $Eu(hfa)_3(TPPO)_2$-beads or $Eu(tta)_3(TPPO)_2$-beads (thickness = 0.5 mm), silicon solar cell (thickness = 0.2 mm), solar cell sealing film without PMMA beads (thickness = 0.5 mm) and a polyvinyl fluoride film (thickness = 0.35mm) were laminated. Prepared materials were heated to 150 ^{o}C under vacuum, and pressing for 20 min using Module laminator. The resultant laminators were used as solar cell module for measurement of solar cell module output.

2.8. Optical Measurements

Absorption spectra of the lanthanide complexes were obtained with JASCOV-670 spectrometer. Emission spectra were measured with a JASCO F-6300-H spectrometer and corrected for the response of the detector system. The emission quantum yields of lanthanide complex solutions degassed with argon (10 mM in acetone-d_6) were obtained by comparison with the integrated emission signal (550–750 nm) of $Eu(hfa)_3(TPPO)$ as a reference (Φ = 0.65: 25 mM in acetone-d_6) with an excitation wavelength of 465 nm (direct excitation of Eu(III) ions) for Eu(III) complexes [15].

3. Result and discussion

3.1 Photophysical properties of Eu(III) complexes and luminescent beads

$Eu(hfa)_3(TPPO)_2$ was synthesized by the ligand exchange reaction of TPPO with $Eu(hfa)_3(H_2O)_2$ and in methanol, according to our previous report [15]. On the other hand, $Eu(tta)_3(TPPO)_2$ was prepared by the complexation of TPPO, tta ligands and europium chloride in mixed solvent of water/isopropano under room temperature. Their chemical structures were identified by using NMR measurements, IR spectroscopies and elemental analyses. Their Eu(III) complexes are composed of three diketonate ligands and two TPPO ligands.

The steady-state emission and excitation spectra of the $Eu(hfa)_3(TPPO)_2$ and $Eu(tta)_3(TPPO)_2$ in acetone-d_6 are shown in Figure 2a. Emission bands for the Eu(III) complexes are observed at ca. 578, 592, 613, 650, and 698 nm and are attributed to the 4f–4f transitions of $^5D_0$–^7F_J with J = 0, 1, 2, 3, and 4, respectively. The spectra are normalized with respect to the magnetic dipole transition intensities at 592 nm ($^5D_0$–$^7F_1$), which is known to be insensitive to the surrounding environment of the lanthanide ions [14]. The emission bands at 613 ($^5D_0$–$^7F_2$ transition) and 700 nm ($^5D_0$–$^7F_4$ transition) are attributed to the electric dipole transition, which is strongly dependent on the

coordination geometry. Notably, the electric dipole transition of $Eu(tta)_3(TPPO)_2$ at 613 nm is more intense than that of $Eu(hfa)_3(TPPO)_2$, which indicates that the coordination symmetry of $Eu(tta)_3(TPPO)_2$ is slightly lower (more asymmetric) than that of $Eu(hfa)_3(TPPO)_2$ in solution. The wavelength of excitation spectra is dependent of the energy gap between π (HOMO) and π^* (LUMO) orbital of diketonate ligands. The energy gap of $Eu(tta)_3(TPPO)_2$ is smaller than that of $Eu(hfa)_3(TPPO)_2$ because of thienyl unit in $Eu(tta)_3(TPPO)_2$. We also observed that absorption coefficient of $Eu(tta)_3(TPPO)_2$ was larger than that of $Eu(hfa)_3(TPPO)_2$ (Table 1). Larger absorption coefficient and red-shift of $Eu(tta)_3(TPPO)_2$ might be due to expansion of π–orbital by thienyl group in the diketonate ligands.

The time-resolved emission profiles of the Eu(III) complexes and luminescent beads revealed single-exponential decays with lifetimes in the millisecond timescale as shown in Figure 2b. The emission lifetimes were determined from the slopes of the logarithmic plots of the decay profiles. The emission quantum yields ($\Phi_{f\text{-}f}$), emission lifetimes (τ_{obs}), radiative (k_r) and nonradiative (k_{nr}) rate constants are summarized in Table 1. The emission quantum yield of $Eu(hfa)_3(TPPO)_2$ (65 %) is two times larger than that of $Eu(tta)_3(TPPO)_2$ (30 %). The highly emission quantum yield of $Eu(hfa)_3(TPPO)_2$ is based on the smaller k_{nr} (2.6×10^2 s^{-1}), which is directly linked to the suppression of vibrational relaxation using low-vibrational frequency hfa ligands [8a]. We suggest that luminescence properties of $Eu(hfa)_3(TPPO)_2$ might be superior to those of $Eu(tta)_3(TPPO)_2$ as a luminescent material.

3.2. Estimation of Thermo- and photo-stability of luminescent beads

In order to protect Eu(III) complex from acidic materials in EVA, $Eu(hfa)_3(TPPO)_2$ was covered with PMMA matrix. The protection of Eu(III) complexes using PMMA expected to provide enhancement of stability in EVA films for solar cell. The SEM image is shown in Figure 3a. We

observed spherical shapes of PMMA beads with $Eu(hfa)_3(TPPO)_2$. From the elemental analysis using EDX measurement, we found the Eu-ions in PMMA beads. The average diameter of the beads was estimated to be 71.8 μm.

The thermo-stability of EVA thin films containing $Eu(hfa)_3(TPPO)_2$ with and without PMMA protection on the silica-glass substrate were examined under air at 120 °C. The time-dependence profiles of the emission intensity of the films excited at 325 nm are shown in Fig. 4a. We observed drastic decrease of emission intensity of EVA thin films with $Eu(hfa)_3(TPPO)_2$ without PMMA protection. The decrease is based on the degradation of $Eu(hfa)_3(TPPO)_2$ in EVA films. The degradation of Eu(III) complex might be caused by incidence of acetic acid under hydrolysis reaction of EVA at 120 °C. After 100 hours under annealing treatment at 120 °C, the emission of EVA film containing $Eu(hfa)_3(TPPO)_2$ has not been observed. In contrast, we found that few decrease of the emission intensity of EVA containing $Eu(hfa)_3(TPPO)_2$ covered with PMMA, $Eu(hfa)_3(TPPO)_2$-beads. The effective thermal stability was achieved by PMMA protection shells around $Eu(hfa)_3(TPPO)_2$ molecules. We here note that glass transition temperature Tg of PMMA is approximately 70 °C. The small decrease of the emission intensity of EVA containing $Eu(hfa)_3(TPPO)_2$-beads might be due to diffusion of acid materials in gel-state PMMA at 120 °C. Luminescent $Eu(hfa)_3(TPPO)_2$-beads may be stable without decomposition under 60 °C (see supporting information Figure S1).

The time-dependence profiles of emission intensities of EVA thin films containing luminescent $Eu(hfa)_3(TPPO)_2$ and $Eu(tta)_3(TPPO)_2$ beads under UV irradiation (Xenon lamp: 60W/m^2) are also shown in Fig. 4b. The emission intensity of EVA thin films with luminescent $Eu(tta)_3(TPPO)_2$ was drastically decrease with increase of the irradiation time, quickly. The decease is caused by degradation of thienyl group in the diketonate ligands. Thienyl group is decomposed by the photochemical oxidation under air [16]. The degradation of thienyl group can be observed using

decrease of the absorption band of tta ligands. Luminescent $Eu(hfa)_3(TPPO)_2$ beads without thienyl group shows slight decrease of the emission intensity under 100 hours.

Here, We calculated the durable lifetime of $Eu(hfa)_3(TPPO)_2$-beads under UV day-light simulators (UV-B: 280-315 nm; artificial lamp composed of metal halide (86.3 w/m^2), super-xenon (18.3 w/m^2) and xenon (6.1 w/m^2)). Durable lifetime of luminescent materials is defined as time until the emission intensity decreases 10%. Based on the calculation, the durable lifetime of luminescent $Eu(hfa)_3(TPPO)_2$ under outdoor exposure for industrial test is estimated to be ten years under air. We also found that the photo-stability of $Eu(hfa)_3(TPPO)_2$-beads is twenty times larger than that of $Eu(tta)_3(TPPO)_2$-beads. We have successfully prepared thermo- and photo-stable Luminescent $Eu(hfa)_3(TPPO)_2$-beads in EVA thin films.

3.4 Performance of $Eu(hfa)_3(TPPO)_2$-beads for of solar cell modulation

EVA is generally used as a surface protector for silicon solar cells. EVA films containing $Eu(hfa)_3(TPPO)_2$-beads are expected to be useful in application for enhancement of energy conversion efficiency of silicon solar cells. In order to estimate the performance of EVA films containing $Eu(hfa)_3(TPPO)_2$-beads for solar cells, prepared EVA thin films were attached on the silicon solar cells. Configuration of the solar cell module with EVA films is shown in Fig. 5a. Finally, iron glass plate is attached to the front surface of solar cell with EVA for protection solar cells from natural hails and dirts under outdoors. Using this module, we carried out the measurement of short-circuit current efficiency. The short-circuit current efficiency of solar cell module under solar simulator are shown in Fig. 5b. The short circuit currents are normalized at silicon solar cell without EVA films. Short circuit current of solar module containing luminescent $Eu(hfa)_3(TPPO)_2$ beads were found to be approximately 1.02. We have observed increase of 2 % of the solar cell short circuit current, totally. The magnitude of increase efficiency is larger than

those of recent solar cell with wavelength converters [18]. Luminescent $Eu(hfa)_3(TPPO)_2$ beads in EVA is effective for enhancement of solar energy conversion efficiency of general silicon solar cells.

4. Conclusions

Photo- and thermo-stable luminescent beads composed of $Eu(hfa)_3(TPPO)_2$ and PMMA were successfully prepared for improvement of silicon solar cells. The stability for outdoor exposure test is estimated to be 10 years. The remarkable stability is based on introduction of photo-stable $Eu(hfa)_3(TPPO)_2$ and protection of PMMA from acid materials in EVA films. The EVA containing $Eu(hfa)_3(TPPO)_2$ beads are expected to be used as a effective protection and improvement film for solar cell under highly temperature and humidity conditions.

Reference

[1] a) G. Blasse, B. C. Grabmaier, Luminescent Materials, Springer-Verlag, New York, (1994) b) A. Vogler, H. Kunkely, Luminescent Metal Complexes: Diversity of Excited States, in: Topics in Current Chemistry, vol. 213, Transition Metal and 511 Rare Earth Compounds (Ed.: H. Yersin), Springer-Verlag, New York (2001).

[2] a) R. Gao, D. G. Ho, B. Hernandez, M. Selke, D. Murphy, P. I. Djurovich, M. E. Thompson, J. Am. Chem. Soc. 124, (2002) 14828–14829; b) J. Li, P. I. Djurovich, B. D. Alleyne, M. Yousufuddin, N. N. Ho, J. C. Thomas, J. C. Peters, R. Bau, M. E. Thompson, Inorg. Chem. 44 (2005) 1713–1727; c) X.-M. Yu, G.-J. Zhou, C.-S. Lam, W.-Y. Wong, X.-L. Zhu, J.-X. Sun, M. Wong, H.-S. Kwok, J. Organomet. Chem. 693 (2008) 1528–1527.

[3] a) B. K. Kaletas, R. M. Williams, B. Konig, L. De Cola, Chem. 521 Commun. (2002) 776–777; b) S. S. Sun, A. J. Lees, P. Y. Zavalij, Inorg. Chem. 42 (2003) 3445–3453.

[4] M. Tropiano, N. L. Kilar, M, Morton, H. Rahman, J. J. Davis, P. D. Beer, S. Faulkner, J. Am. Chem. Soc. 133 (2011) 11847-11849.

[5] L.D.Carlos, Rute A. S. Ferreira, Veronica de Zea Bermudez, Beatriz Julian-Lopez, Purification Escribano, Chem. Soc. Rev. 40 (2011) 536-549.

[6] S. V. Eliseeva, Jean-Claude G. Bünzli, Chem. Soc. Rev. 39 (2010) 189-227.

[7] a) Jean-Claude G. Bünzli, Chem. Rev. 110 (2010) 2729-2755; b) D. Parker, R. S. Dickins, H. Puschmann, C. Crossland, and J. A. K. Howard, Chem. Rev. 102 (2002) 1977-2010.

[8] a) Y. Hasegawa, Y. Kimura, K. Murakoshi, Y. Wada, J. Kim, N. Nakashima, T. Yamanaka, S. Yanagida, J. Phys. Chem. 100 (1996) 10201–10205; b) K. Nakamura, Y. Hasegawa, H. Kawai, N. Yasuda, N. Kanehisa, Y. Kai, T. Nagamura, S. Yanagida, Y. Wada, J. Phys. Chem. A 111 (2007,) 3029–3037; c) Y. Hasegawa, S. Tsuruoka, T. Yoshida, H. Kawai, T. Kawai, J. Phys. Chem. A 112 (2008) 803–807; d) K. Miyata, T. Nakagawa, R. Kawakami, Y. Kita, K. Sugimoto, T. Nakashima, T. Harada, T. Kawai, Y. Hasegawa, Chem. Eur. J. 17 (2011) 521–528; e) S. Kishimoto, T. Nakagawa, T. Kawai, Y. Hasegawa, Bull. Chem. Soc. Jpn. 82 (2011) 148–154; f) K. Miyata, Y. Konno, T. Nakanishi, A. Kobayashi, M. Kato, K. Fushimi, Y. Hasegawa, 641 Angew. Chem. Int. Ed. 52 (2013) 6413–6416.

[9] Recent selected papers of luminescent lanthanide complexes: a) D. Sykes, M. D. Ward, Chem. Commun. 47 (2011) 2279–2281; b) M. Sturzbecher-Hoehne, C. N. P. Leung, A. D'Aléo, B. Kullgren, A.-L. Prigent, D. K. Shuh, K. N. Raymond, R. J. Abergel, Dalton Trans. 40 (2011) 8340–8346; c) C. M. Andolina, J. R. Morrow, Eur. J. Inorg. Chem. (2011) 154–164; d) J. Andres, A.-S. Chauvin, Inorg. Chem. 50 (2011) 10082–10090; e) Q.-B. Bo, H.-Y. Wang, D.-Q. Wang, Z.-W. Zhang, J.-L. Miao, G.-X. Sun, Inorg. Chem. 50 (2011) 10163–10177; f) S. V. Eliseeva, D. N. Pleshkov, K. A. Lyssenko, L. S. Lepnev, J.-C. G. Bünzli, N. P. Kuzmina, Inorg. Chem. 50 (2011) 5137–5144; g) J. An, C. M. Shade, D. A. Chengelis-Czegan, S. Petoud, N. L. Rosi, J. Am.

Chem. Soc. 133 (2011) 1220–1223; h) D. J. Lewis, P. B. Glover, M. C. Solomons, Z. Pikramenou, J. Am. Chem. Soc. 133 (2011) 1033–1043; i) M. Varlan, B. A. Blight, S. Wang, Chem. Commun. 48 (2012) 12059–12061; j) D. G. Smith, B. K. McMahon, R. Pal, D. Parker, Chem. Commun. 48 (2012) 8520– 8522; k) R. M. Edkins, D. Sykes, A. Beeby, M. D. Ward, Chem. Commun. 48 (2012) 9977–9979; l) A. Nonat, M. Regueiro-Figueroa, D. Esteban-Gomez, A. de Blas, T. Rodríguez-Blas, C. Platas-Iglesias, L. J. Charbonnière, Chem. Eur. J. 18 (2012) 8163–8173; m) S. Nadella, P. M. Selvakumar, E. Suresh, P. S. Subramanian, M. Albrecht, M. Giese, R. Frohlich, Chem. Eur. J. 18 (2012) 16784–16792; n) D. G. Smith, R. Pal, D. Parker, Chem. Eur. J. 18 (2012) 11604–11613; o) E. S. Andreiadis, D. Imbert, J. Pécaut, R. Demadrille, M. Mazzanti, Dalton Trans. 41 (2012) 1268–1277; p) D. J. Lewis, F. Moretta, A. T. Holloway, Z. Pikramenou, Dalton Trans. 41 (2012) 13138–13146; q) Y.-A. Li, S.-K. Ren, Q.-K. Liu, J.-P. Ma, X. Chen, H. Zhu, Y.-B. Dong, Inorg. Chem. 51 (2012) 9629–9635; r) S. Mohapatra, S. Adhikari, H. Riju, T. K. Maji, Inorg. Chem. 51 (2012) 4891–4893; s) A. R. Ramya, D. Sharma, S. Natarajan, M. L. P. Reddy, Inorg. Chem. 51 (2012) 8818–8826; t) A. de Bettencourt-Dias, P. S. Barber, S. Bauer, J. Am. Chem. Soc. 134 (2012) 6987–6994; u) M. O. Rodrigues, J. D. L. Dutra, L. A. O. Nunes, G. F. de Sá, W. M. de Azevedo, P. Silva, F. A. A. Paz, R. O. Freire, S. A. Júnior, J. Phys. Chem. C 116 (2012) 19951–19957; v) K.-N. T. Hua, J. Xu, E. E. Quiroz, S. Lopez, A. J. Ingram, V. A. Johnson, A. R. Tisch, A. de Bettencourt-Dias, D. A. Straus, G.Muller, Inorg. Chem. 51 (2012) 647–660; w) A. Ablet, S.-M. Li, W. Cao, X.-J. Zheng, W.-T. Wong, L.-P. Jin, Chem. Asian J. 8 (2013) 95–100; x) J. Xu, L. Jia, N. Jin, Y. Ma, X. Liu, W. Wu, W. Liu, Y. Tang, F. Zhou, Chem. Eur. J. 19 (2013) 4556–4562; y) N. Wartenberg, O. Raccurt, E. Bourgeat-Lami, D. Imbert, M. Mazzanti, Chem. Eur. J. 19 (2013) 3477–3482.

[10] T. Jin, S. Inoue, K. Machida, G. Adachi, J. Electrochem. Soc. 144 (1997) 4054-4058.

[11]T.Fukuda, S.Kato, E.Kin, K.Okaniwa, H.Morikawa, Z.Honda, N.Kamata, Opt. Mater. 32,

(2009) 22-25.

[12] M. Segawa, MATERIAL STAGE 9 (2009) 92-94.

[13] K. Kawano, MATERIAL STAGE 12, (2009) 40-46.

[14] N. Kamata, Function and Materials 30 (2011) 31-37.

[15] Y. Hasegawa, M. Yamamuro, Y. Wada, N. Kanehisa, Y. Kai, S. Yanagida, J. Phys. Chem. A, 107 (2003) 1697–1702.

[16] P. Nockemann, E. Beurer, K. Driesen, R. V. Deun, K. V. Hecke, L. V. Meervert, K. Binnemans, Chem. Commun. (2005) 4354-4356.

[17] L. A. Escobar, W. Q. Meeker, Statical Science 21 (2006) 552-577.

[18] D. Fujishima, A. Yano, T. Kinoshita, M. Taguchi, E. Maruyama, M. Tanaka, Panasonic Technical Journal 57 (2012) 40-45.

Figure caption

Figure 1. Chemical structures of a) $Eu(hfa)_3(TPPO)_2$ and b) $Eu(tta)_3(TPPO)_2$. c) Preparation scheme of PMMA beads containing Eu(III) complexes.

Figure 2. a) Absorption and emission spectra of $Eu(tta)_3(TPPO)_2$ and $Eu(hfa)_3(TPPO)_2$ in acetone-d_6 at room temperature. Excited at 465 nm. The emission spectra were normalized with respect to the magnetic dipole transition ($^5D_0$-$^7F_1$). b) Emission decays of Eu(III) complexes (1. $Eu(tta)_3(TPPO)_2$ 2. $Eu(hfa)_3(TPPO)_2$ in acetone-d_6). Excited at 532 nm (Nd: YAG 3ω, pulse width = 5 ns).

Figure 3. a) SEM image of luminescent PMMA beads with $Eu(hfa)_3(TPPO)_2$. b) Particle size distribution of luminescent PMMA beads with $Eu(hfa)_3(TPPO)_2$.

Figure 4. Normalized emission stability of EVA film with $Eu(hfa)_3(TPPO)_2$-beads(filled circle) and $Eu(TTA)_2(TPPO)_3$-beads(open circle) at Xenon UV irradiation ($60W/m^2$). b). Normalized emission stability of EVA film with $Eu(hfa)_3(TPPO)_2$-beads with PMMA-coating (filled circle) and $Eu(hfa)_3(TPPO)_2$-beads without PMMA-coating (open circle) under 120 ^oC.

Figure 5. a) Configuration of solar cell module. b) Normalized short-circuit current efficiency of solar cell modules with $Eu(hfa)_3(TPPO)_2$-beads (black circles) and without $Eu(hfa)_3(TPPO)_2$-beads (white circle). Solar cell module without $Eu(hfa)_3(TPPO)_2$-beads (concentration of PMMA beads: 0%) is contained with UV absorber (organic dye) for protection of solar cell module.

Table 1 Absorption and emission properties of Eu(III) complexes

	ε[a] /10^4 $cm^{-1}M^{-1}$	$\Phi_{f\text{-}f}$[b] /%	τ_{obs}[c] /ms	k_r[d] /10^2 s^{-1}	k_{nr}[e] /10^2 s^{-1}
$Eu(hfa)_3(TPPO)_2$	1.6	65	1.33	4.8	2.6
$Eu(tta)_3(TPPO)_2$	4.7	30	0.93	3.3	7.5

a) Absorption coefficients at π–π* transition bands of the diketonate ligands. b) Excited at 465 nm. Concentration: 25 mM (in acetone-d_6). c) Excited at 355 nm (Nd:YAG 3ω). Concentration: 25 mM (in acetone-d_6). d) Radiative rate constant $k_r = \Phi_{f\text{-}f}/\tau_{obs}$. e) Nonradiative rate constant $k_{nr} = 1/\tau_{obs} - k_r$.

H. Kataoka et al, Figure 1

a)

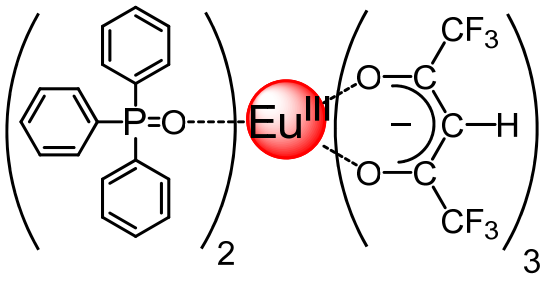

Eu(hfa)$_3$(TPPO)$_2$

b)

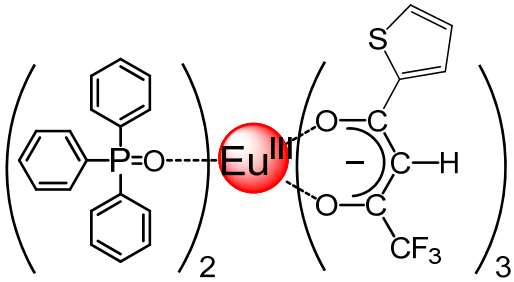

Eu(tta)$_3$(TPPO)$_2$

c)

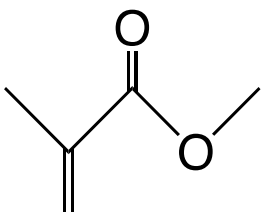

MMA

AIBN, BPO, EOMA
Eu(III) complex

55 ˚C, 1h 90 ˚C, 3h

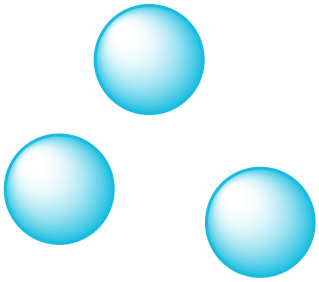

PMMA beads with
Eu(III) complex

H. Kataoka et al, Figure 2

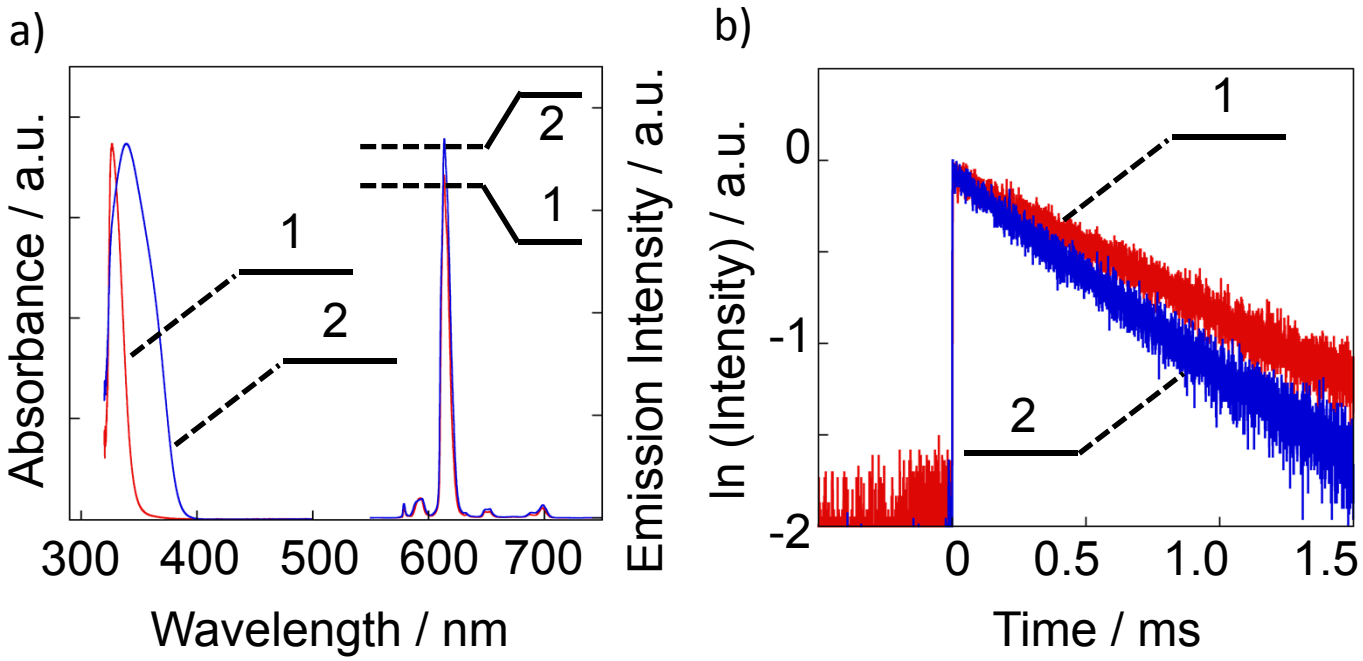

H. Kataoka et al, Figure 3

a)

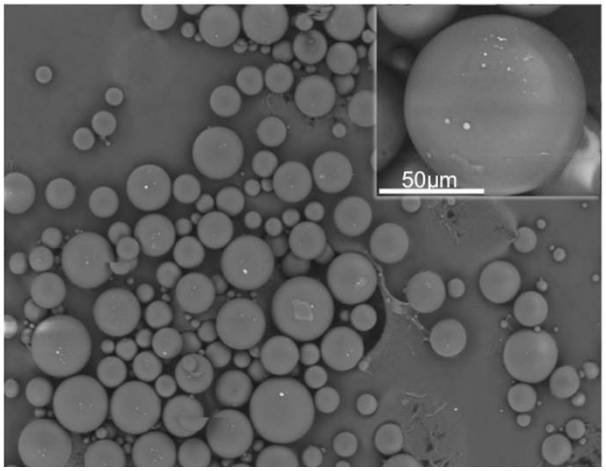

500 μm

b)

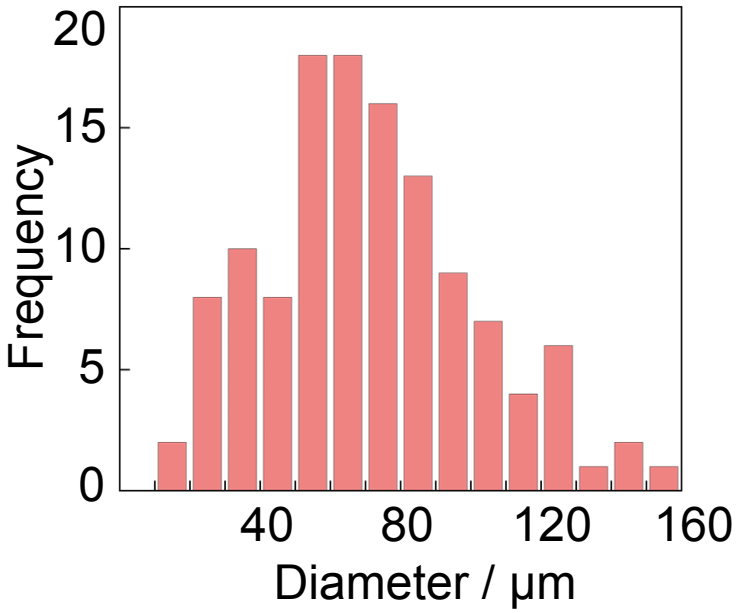

H. Kataoka et al, Figure 4

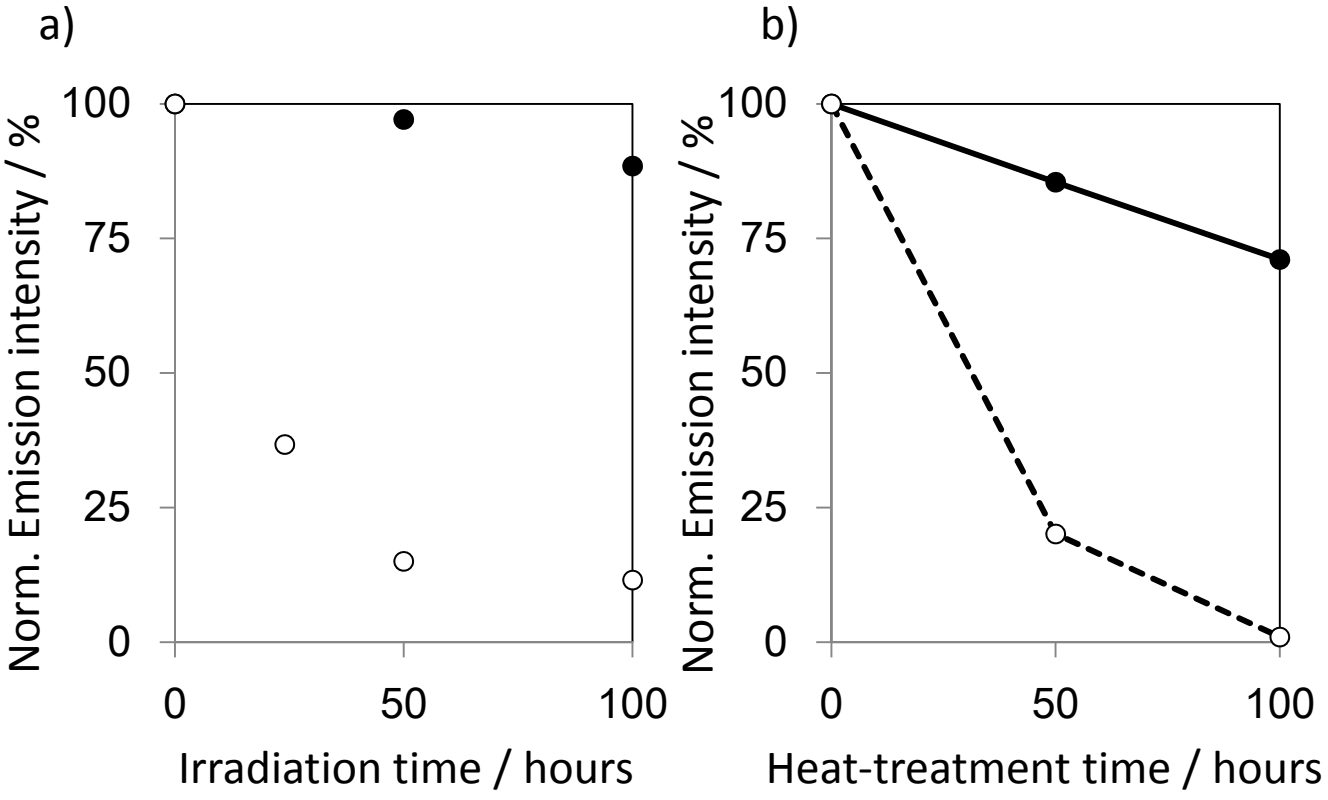

H. Kataoka et al, Figure 5